



Share Your Innovations through JACS Directory

# Journal of Nanoscience and Technology

Visit Journal at <http://www.jacsdirectory.com/jnst>

## A Facile Synthesis of Copper Oxide Nanorods for Photocatalytic Degradation of Organic Pollutant and Inactivation of Pathogens

Sathish Mohan Botsa<sup>1</sup>, Dharmasoth Ramadevi<sup>2</sup>, K. Basavaiah<sup>1,\*</sup><sup>1</sup>Department of Inorganic and Analytical Chemistry, Andhra University, Visakhapatnam – 530 003, Andhra Pradesh, India.<sup>2</sup>AU College of Pharmaceutical Sciences, Andhra University, Visakhapatnam – 530 003, Andhra Pradesh, India.

### ARTICLE DETAILS

#### Article history:

Received 17 July 2018

Accepted 03 August 2018

Available online 07 August 2018

#### Keywords:

Copper Oxide Nanorods

Green Synthesis

Sonochemical Synthesis

Nitrobenzene (NB)

Photocatalysis

Antimicrobial Activity

### ABSTRACT

In the recent years, green synthesis of nanomaterials has received a great attention to researchers in worldwide due to eco-friendly and scalable synthesis. Here, we report a green synthesis of copper oxide (CuO) nanorods via sonochemical assisted approach. The crystalline structure, band gap and morphology of as prepared CuO nanorods were investigated by UV-Vis diffuse reflectance (UV-Vis/DRS), Fourier Transform infrared spectroscopy, powder X-Ray diffraction (XRD) pattern and scanning electron microscopy (FESEM-EDX). The bandgap of as prepared CuO nanorods was found to be 2.0 eV, which falls in the visible region of solar spectrum. FTIR demonstrated that there is strong interaction between Cu and oxygen in prepared CuO. XRD results reveal the formation of phase pure and crystalline CuO. FESEM images clearly show the rod-like morphology of CuO and the presence of elemental copper and oxygen in EDX, confirms the formation of CuO. The photocatalytic degradation activity of CuO nanorods was examined against a model dye pollutant, nitrobenzene (NB) under visible light irradiation. CuO nanorods effectively degraded the NB under visible light irradiation. CuO nanorods act as a potent and show enhanced antimicrobial activity against pathogenic fungi, *Candida albicans* and bacteria, *Escherichia coli*.

### 1. Introduction

During the past two decades, a large quantity of heavy metals and toxic organic pollutants such as synthetic dyes, pesticides, fertilizers, hydrocarbons, phenols, biphenyls, plasticizers, detergents and oils etc have been released into an aquatic environment, from industrial effluents, agriculture waste water, municipal waste water and other environmental changes [1, 2]. Especially, bioaccumulated organic pollutants show potential adverse impact on human as well as aquatic life. Among all organic pollutants, carcinogenic and toxic nitrobenzene (NB) has been a great threat to human health. Moreover, NB is stable and resistant to biological or chemical oxidation due to the presence of strong electron affinity nitro group of NB [3]. Therefore it is highly desirable to remove or degrade highly toxic organic pollutants from contaminated water.

There were number of traditional water treatment methods including physical, chemical and biological techniques such as adsorption, coagulation and membrane separation have been developed for removal of dyes from water. However, all these techniques suffer from high operating costs and generate secondary pollutants [4]. More recently, semiconductor heterogeneous photocatalysis has emerged as an alternative potential tool for reduction of organic pollutant without generation of any secondary pollutants. Especially, semiconductor photocatalysts such as TiO<sub>2</sub>, ZnO, Fe<sub>2</sub>O<sub>3</sub>, CdS, GaP, ZnS and CuO [5-9] have been extensively used for degradation of wide range of organic dye pollutants. Among heterogeneous semiconductor photocatalysts, CuO has been received a special attention for catalytic degradation of organic dye pollutant under visible light radiation due to its non-toxicity, ease of preparation, its unique physical, optical and electrical properties and tunable narrow bandgap (2.1 eV) [10].

Numerous methods have been reported for preparation of CuO nanostructures such as precipitation, thermal oxidation and combustion [11]. However, all these methods used toxic chemical and thus limits CuO applications in pollution abatement and biomedical applications. More recently, sonochemical method has been proven as versatile and green route to synthesize the wide range of materials such as metal, oxide,

carbide and sulphide nanorods [12-15] due to a simple, rapid, cost-effective and environmentally benign [16].

Herein, we report sonochemical assisted synthesis of CuO nanorods by hydrolysis of copper (II) sulphate in presence of sodium hydroxide and hydrazine sulphate as reducing agent. The photocatalytic activity of as prepared CuO nanorods was investigated against NB. Antimicrobial activity of CuO nanorods were also investigated against *Candida albicans* and *E. coli*.

### 2. Experimental Methods

#### 2.1 Materials

The chemicals such as copper acetate Cu(CH<sub>3</sub>COO)<sub>2</sub>, sodium hydroxide (NaOH) and hydrazine sulphate (NH<sub>2</sub> NH<sub>2</sub>.H<sub>2</sub>SO<sub>4</sub>) received from Sigma Aldrich. Nitrobenzene (99%) was obtained from Sigma Aldrich and used without further purification. Doubly distilled water was used throughout the experiments. All the aforementioned chemicals were of analytical reagent grade and used without further purification.

#### 2.2 Synthesis of Copper Oxide Nanorods

In a typical synthesis, 100 mL of 0.25 M Cu(CH<sub>3</sub>COO)<sub>2</sub> was taken in a beaker and ultrasonicated for 10 minutes. Then, a 100 mL of 1 M NaOH was added to above solution and ultrasonicated (probe ultrasonicator, sonics vibra cell, 20 kHz, 50% amplitude) for 10 minutes. The reaction mixture was turned into dark intense green colour. Then 0.014 g of NH<sub>2</sub>.NH<sub>2</sub>.H<sub>2</sub>SO<sub>4</sub> was added to the reaction mixture under ultrasonication for 30 minutes. A dark colour precipitate was obtained which indicates the formation of CuO nanorods. Finally, the precipitate was filtered, washed and dried under vacuum at room temperature.

#### 2.3 Characterization

UV-Visible absorption and diffuse reflectance spectra were recorded by UV-Visible diffuse reflectance spectrometer (Shimadzu-2600R) in the range of 200-800 nm. FT-IR (IR Prestige21, Shimadzu, Pvt Ltd, Japan) spectra of the samples in KBr pellets were obtained on a Shimadzu spectrometer in the range of 400-4000 cm<sup>-1</sup>. The powder X-Ray diffraction

\*Corresponding Author: kbasu@gmail.com (K.Basavaiah)

(XRD) was recorded using Cu K $\alpha$  radiation at 30.0 kV and 30.0 mA over the scan range 2 $\theta$ , 10–80° at scan rate of 2° min<sup>-1</sup>. Morphology of CuO Nanorods was investigated by field emission scanning electron microscopy (FESEM, JSM-6610LV, Jeol Asia PTE Ltd, Japan) and the elemental analysis was conducted by EDX.

### 2.4 Photocatalytic Degradation of NB

Photocatalytic activity of CuO nanorods was evaluated in terms of degradation of NB under visible light. In typical, 50 mg of CuO was added to 100 mL NB aqueous solution (15 mg/L) and then the solution was stirred for 30 minutes in dark to ensure adsorption-desorption equilibrium between CuO nanorods and NB. The solution was then exposed to 400 W metal halide lamp and then samples (5 mL) were collected from the reaction vessel and centrifuged at 2000 rpm for 30 min to recover the photocatalyst. Photocatalytic experiments were conducted in photoreactor system in presence of visible light source and 20 cm distance maintained between light source and reaction vessel. The reaction vessel is surrounded with water system to keep the photocatalytic reaction system at ambient temperatures and to absorb the IR radiation.

The percentage of degradation of dye in presence of CuO was investigated by a UNICAM UV 500, UV-visible spectrophotometer (Thermo Electron Corporation, India). Photodegradation efficiency was reported by plotting  $C/C_0$  vs irradiation time (min), where  $C_0$  and  $C$  are the NB dye concentrations at zero time and time 't' respectively. The value of  $C/C_0$  was taken as the ratio  $A/A_0$ , i.e. the absorbance of the solution at  $\lambda_{max}$  at time t divided by the absorbance at time zero (for NB  $\lambda_{max}$  = 280 nm).

$$\text{Photodegradation \%} = \frac{C_0 - C_t}{C_0} \times 100$$

where  $C_0$  and  $C_t$  corresponds to the initial absorbance and absorbance at time 't' respectively.

### 2.5 Investigation of Antimicrobial Activity

The antimicrobial activity was carried out by employing 24 h young cultures with the given compounds by using agar well diffusion method. The medium was sterilized by autoclaving at 120 °C (15 lb/in<sup>2</sup>). About 20 mL of the medium (Nutrient Agar Medium) with the respective bacterial strains of bacteria and medium (potato dextrose agar) for fungal strains were transferred aseptically into each sterilized Petri plate. The plates were allowed to cool at room temperature for solidification. Each plate was made into 5 wells with equal distance of 6mm sterile borer. The test CuO nanorods were freshly reconstituted in dimethylsulfoxide (DMSO) and tested at various concentrations. The samples and the control along with standard (Ciprofloxacin) were placed in 6-mm diameter well. In Antimicrobial assays plates were incubated at 28 ± 2 °C for fungi about 24 h and 37 ± 2 °C for bacteria 12 h. Standard with 5 µg/mL was used as a positive control for antibacterial activity. Activity diameter of the zone of inhibition was measured using antibiotic zone scale.

## 3. Results and Discussion

### 3.1 UV-Vis Diffuse Reflectance Spectroscopy (UV-Vis/DRS)

The UV-Vis/DRS spectrum of CuO nanorods is depicted in Fig. 1(a). The band gap of CuO nanorods was calculated from diffuse reflectance spectra by using Eq.(1),

$$E_g = h\nu = hc/\lambda = 1240/\lambda \quad (1)$$

where  $E_g$  is bandgap energy,  $h$  is planks constant,  $\nu$  is wave frequency,  $c$  is light of speed and  $\lambda$  is the wavelength. The band gap of CuO nanorods found to be 2.06 eV, which is fall in the visible region of solar spectrum and therefore CuO nanorods could be utilized as an efficient photocatalyst in visible region of solar spectrum.

### 3.2 X-Ray Diffraction Patterns (XRD)

The XRD patterns of CuO nanorods were presented in Fig. 1(b). The diffractions peaks centered at 32.67°, 35.71°, 38.88°, 49.01°, 53.45°, 58.41°, 61.69°, 66.35°, 68.28°, 72.29° and 75.23°, which are assigned to be (110), (111), (111), (202), (020), (202), (113), (310), (220), (221) and (222) plane of CuO nanorods. The XRD patterns of CuO nanorods well in arrangement with the standard JCPDS file (No.96-410-5686) [17]. The average crystallite size of prepared CuO nanorods was calculated by Debye-Scherrer's equation and found to be 27.62 nm.

<https://doi.org/10.30799/jnst.146.18040502>

Cite this Article as: Sathish Mohan Botsa, Dharmasoth Ramadevi, K. Basavaiah, A facile synthesis of copper oxide nanorods for photocatalytic degradation of organic pollutant and inactivation of pathogens, J. Nanosci. Tech. 4(5) (2018) 467–470.

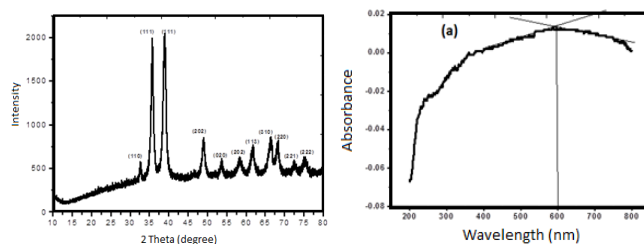


Fig. 1 (a) UV-Vis diffuse reflectance spectra and (b) The powder XRD patterns of CuO nanorods

### 3.3 FTIR Spectroscopy

FTIR spectrum of CuO nanorods was depicted in Fig. 2, which is well in agreement with the reported literature. The characteristic bands at 605 and 668 cm<sup>-1</sup> ascribed to Cu(II)-O stretching frequencies respectively [18]. There is sharp peak observed at 605 cm<sup>-1</sup> in the spectrum is due to characteristics of Cu-O bond formation in CuO. The broad absorption band at around 3427 cm<sup>-1</sup> is caused by the adsorbed water molecules. Three intense bands were centered at 1384.34 cm<sup>-1</sup>, 1028.92 cm<sup>-1</sup> and 1545.73 cm<sup>-1</sup> are attributed to the stretching vibrations of C=O, C=C and C-H groups respectively, which suggests its presents as adsorbed species in the surface of nanorods [19].

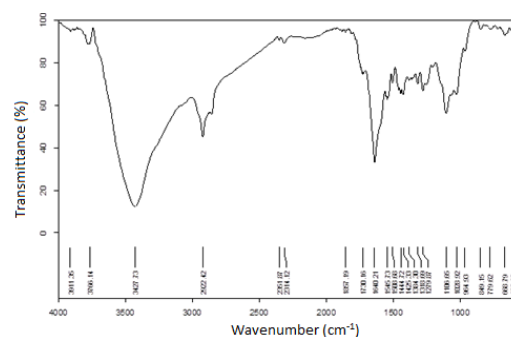


Fig. 2 FT-IR spectra of CuO nanorods

### 3.4 Morphology

The morphology of as prepared CuO nanorods was investigated by FESEM. The representative FESEM images and EDX spectrum of CuO nanorods was presented in Fig. 3. FESEM images clearly show the rod like structure. The presence of elemental copper (Cu) and oxygen (O) in the EDX spectrum confirms the formation of CuO nanorods via sonochemical method. The synthesized CuO are nearly rod-like structure with average diameter ranges from 18-30 nm.

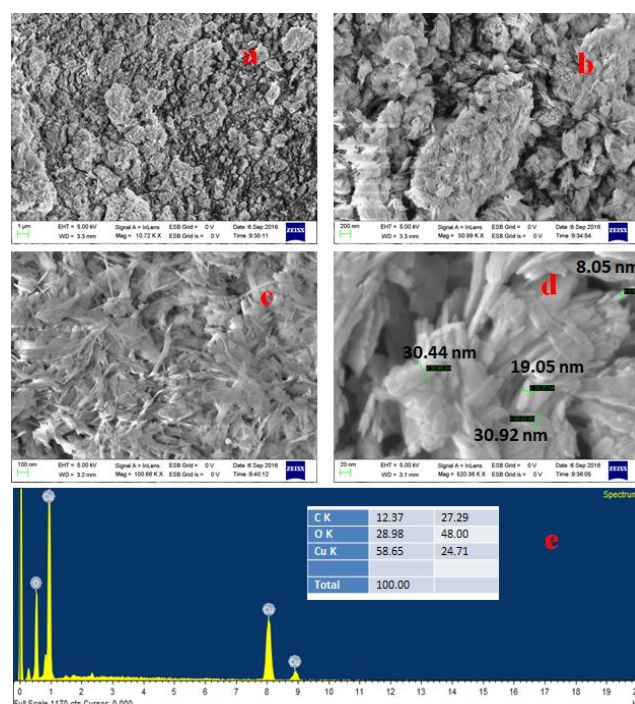


Fig. 3 (a-d) FESEM images and (e) EDX spectrum of CuO nanorods

### 3.5 Raman Analysis

The Raman spectrum of prepared CuO NPs is presented in Fig. 4. The spectrum shows characteristic Raman bands at 290, 336 and 302  $\text{cm}^{-1}$  [20–22] which are in good agreement with reported literature for metal oxides such as CuO.

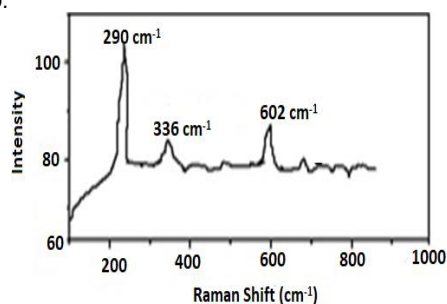


Fig. 4 Raman spectrum of prepared CuO nanorods

### 3.6 Photocatalytic Degradation of NB using CuO Nanorods

In presence of CuO nanorods, NB was successfully photodegraded under visible light irradiation. In general, photocatalytic degradation of NB is depended on various experimental conditions such as catalyst dose, pH of reaction medium and NB concentration. In order to know the best degradation conditions; the degradation was carried out at different experiments. Initially, NB was subjected to visible light radiation for 150 minutes and NB was not degraded under visible light irradiation. There was a significant degradation of NB in presence of CuO nanorods as photocatalyst, which is further confirmed by calculating the normalized change in the concentration of NB before and after light irradiation ( $C/C_0$ ).

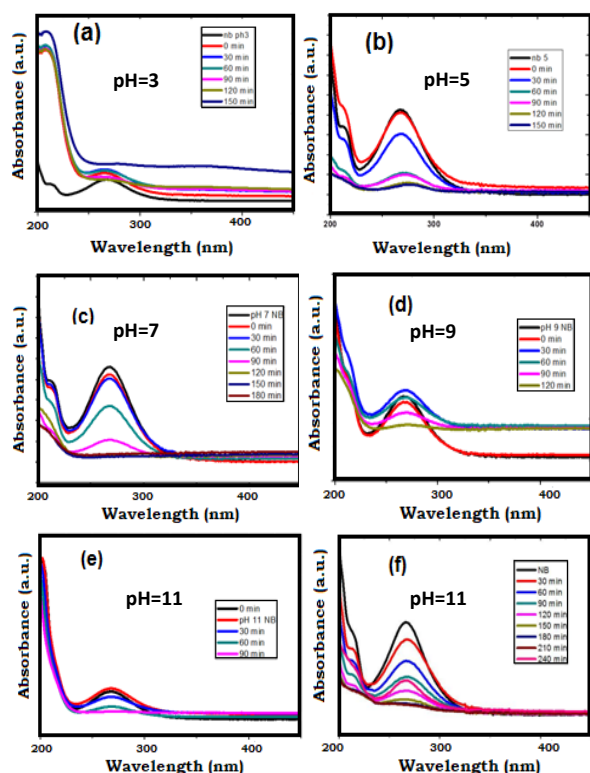


Fig. 5 Photocatalytic activity of CuO towards the degradation of NB under visible light irradiation at (a-e) different pH and (f) Only NB

#### 3.6.1 Effect of pH on Degradation of NB

The surface of CuO is critically depending on pH of reaction medium. The point of zero charge ( $P_{zc}$ ) for CuO particles is 6.8, so there is an electrostatic absorption between positive charge surfaces of CuO and the dye. As the pH of the system increases, the number of surfaces with negative charge increases on surface of CuO. The effect of variation of pH of reaction system on photocatalytic degradation was evaluated at constant NB concentration (15 mg/L) by varying the pH from 3, 5, 7, 9 and 11. The degradation efficiencies of NB follows the order  $\text{pH}=7 > \text{pH}=5 > \text{pH}=11 \approx \text{pH}=9 > \text{pH}=3$  with percentages of dye degradation are 94.5, 89, 74, 51 and 23% respectively (Fig. 5). The highest photocatalytic degradation of NB by CuO nanorods was observed at  $\text{pH}=7$  with a degradation efficiency of 94.5%.

<https://doi.org/10.30799/jnst.146.18040502>

#### 3.6.2 Effect of Catalyst Dose on Degradation of NB

The amount of catalyst dose is critically influence the photocatalytic degradation of NB. In order to investigate the optimum concentrate of CuO, the photocatalysis was carried out at different amounts of CuO (10 mg, 20 mg and 30 mg) while the concentration (15 mg/L) of NB solution kept constant at  $\text{pH}=7$ . The percentage degradation of NB is increased with increase of dose of catalyst up to 30 mg and then degradation rate decreases by increase in dose of CuO (Fig. 6). Hence the optimized dosage of photocatalyst could be 30 mg.

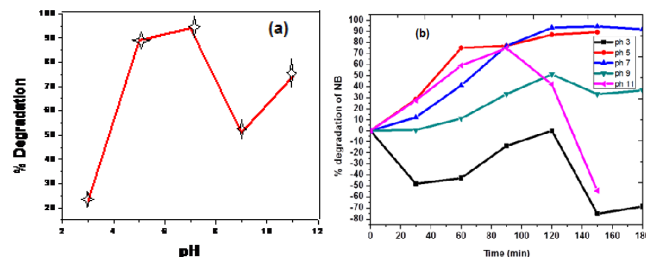


Fig. 6 The percentage of degradation of NB using CuO nanorods (a) under the effect pH and (b) at different time intervals

The rate kinetic also be calculated from photocatalytic reaction and the calculated values are shown in Table 1, which indicates that entire process follows the pseudo first order reaction. The linear relationship between  $\ln(C/C_0)$  and time demonstrates that the pseudo first order kinetics shown in Fig. 7.

$$H = \ln(C/C_0) = kt \quad (2)$$

where ' $C/C_0$ ' is normalized initial concentration, ' $t$ ' is the reaction time, and ' $k$ ' is the reaction rate constant ( $\text{min}^{-1}$ ).

Table 1 First order kinetic rate constant ( $k$ ) and regression coefficient ( $R^2$ ) of NB degradation under visible light irradiation

pH	Nitrobenzene (NB)	
	$k \times 10^{-4}$ in $\text{min}^{-1}$	$R^2$
3	1.025	0.95
5	1.3	0.95
7	1.66	0.98
9	2.02	0.97
11	1.48	0.92

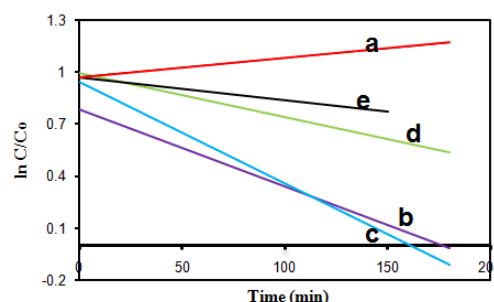


Fig. 7 Plot of  $\ln C/C_0$  vs time at (a)  $\text{pH}=3$ , (b)  $\text{pH}=5$ , (c)  $\text{pH}=7$ , (d)  $\text{pH}=9$ , (e)  $\text{pH}=11$  and (f) Only NB

### 3.7 Antimicrobial Investigation using CuO Nanorods

The antimicrobial activity of CuO nanorods was investigated by well diffusion method. The CuO nanorods showed remarkable antibacterial activity against Gram-negative bacteria, *E. coli* (24 h) and antifungal activity against *C. albicans* (36 h) were shown in Table 2.

Table 2 Shows Bacteria and fungus organism test by CuO nanorods

Compound (Time)	Organism/s	25	10	5
		mg/mL	mg/mL	mg/mL
12 h	<i>E.coli</i>	8	8	-
18 h	<i>E.coli</i>	18	8	8
26 h	<i>E.coli</i>	26	12	8
26 h	<i>C.albicans</i>	22	14	7

Fig. 8 shows the results of the inhibition zone values for CuO against *E. coli* and *C. albicans*. Fig. 9 represents the antibacterial activity achieved 25 mg/mL at 24 h in presence of CuO, shows that the prepared CuO has potential antibacterial application against *E.coli*. The antibacterial activity



of CuO was mainly attributed to adhesion with bacteria because of their opposite electric charges resulting in a reduction at the bacterial cell wall. Large number of antibiotics carried out by CuO nanorods owing to their large surface area.

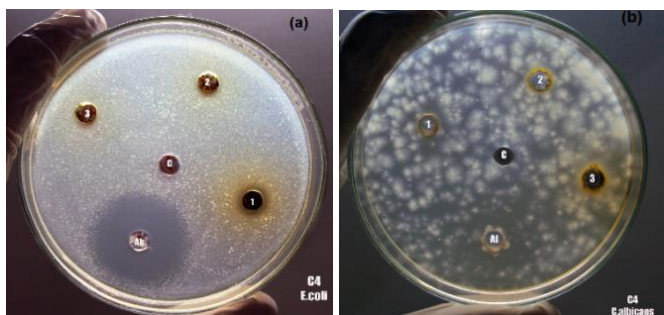


**Fig. 8** Photographic images of inhibition zone produced by CuO nanorods against (a) *E. coli* and (b) *C. albicans*

Antimicrobial activity of CuO NPs studies is very limited. Among the few studies, CuO NPs has antibacterial activity against a range of gram-positive and gram-negative bacteria such as *S. aureus*, Epidemic MRSA-15 and *E. coli* [23]. The silver NPs were studied in most related research, exhibiting antibacterial effect at low concentrations [24]. Ionic nanoparticulate metal oxides are among the potentially interesting antimicrobial agents, because of their extremely high surface areas and having unusual crystalline structures with high number of edges and corners and other reactive sites [25]. CuO nanoparticle is the simplest member of the Cu compounds that reveal a range of potential physical properties and is much cheaper than silver oxide.

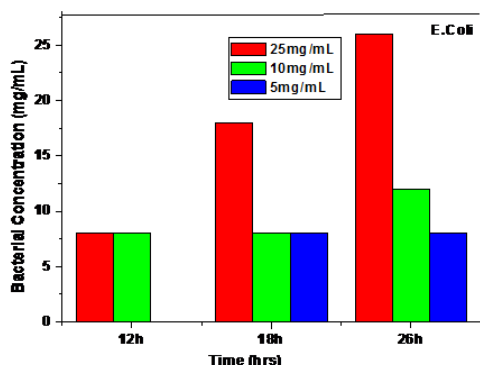


**Fig. 9** Representation of bacterial concentration at different time intervals

#### 4. Conclusion

In conclusion, CuO nanorods were successfully synthesised via simple sonochemical route. The spectroscopic and microscopic results reveal the successful formation of CuO nanorods. The catalytic activity of CuO nanorods was investigated using model dye, NB under visible light irradiation and shows enhanced degradation of NB in a short time. The prepared CuO nanorods shows enhanced antimicrobial activity against *E. coli* and fungi *C. albicans* in 26 h.

#### Acknowledgement

B. Sathish Mohan, grateful to University Grants Commission (UGC) for sponsoring Rajiv Gandhi National Fellowship (RGNF-SC-2016-17-AND-

9309). Also, authors thank to UGC-SAP-DRS-I and DST-FIST in Department of Inorganic and Analytical Chemistry, Andhra University.

#### References

- [1] I. Ali, H.Y. Aboul Enein, Chiral Pollutants: distribution, toxicity and analysis by chromatography and capillary electrophoresis, *J. Am. Chem. Soc.* 126 (44) (2004) 14680-14680.
- [2] Y. Chen, H. Li, W. Liu, Y. Tu, Y. Zhang, W. Han, L. Wang, Electrochemical degradation of nitrobenzene by anodic oxidation on the constructed TiO<sub>2</sub>-NTs/SnO<sub>2</sub>-Sb/PbO<sub>2</sub> electrode, *J. Chemosphere* 113 (2014) 48-55.
- [3] Z.H. Zhang, Y. Yuan, Y.J. Fang, L.H. Liang, H.C. Ding, L.T. Jin, Preparation of photocatalytic nano-ZnO/TiO<sub>2</sub> film and application for determination of chemical oxygen demand, *J. Talanta* 73(2007) 523-528.
- [4] G. Buddhika, S. Naresh, S. Peter, Degradation of Chlorinated phenols by zero valent iron and bimetals of iron: A review, *Environ. Eng. Res.* 16 (2011) 187-203.
- [5] Y. Zhang, Y.P. Li, H.B. Cao, C.M. Liu, Electrochemical reduction of nitrobenzene at carbon nanotube electrode, *J. Hazard. Mater.* 148 (2007) 158-163.
- [6] A. Vogelpohl, S. Sakthivel, S.U. Geissen, D.W. Bahnemann, V. Murugesan, Enhancement of photocatalytic activity by semiconductor heterojunctions:  $\alpha$ -Fe<sub>2</sub>O<sub>3</sub>, WO<sub>3</sub> and CdS deposited on ZnO, *J. Photochem. Photobiol. A* 148 (2002) 283-293.
- [7] C. Haneda, X.M. Wang, B.Q. Wang, J.C. Xu, B.X. Zhao, Mai, H.D. Li, Photocatalysis of sprayed nitrogen-containing Fe<sub>2</sub>O<sub>3</sub>-ZnO and WO<sub>3</sub>-ZnO composite powders in gas-phase acetaldehyde decomposition, *J. Photochem. Photobiol. A* 160 (2003) 203-212.
- [8] A. Henglein, L. Spanhel, H. Weller, Photochemistry of semiconductor colloids. injection from illuminated CdS into attached TiO<sub>2</sub> and ZnO, *J. Am. Chem. Soc.* 109 (1987) 6632-6635.
- [9] J. Rabani, Sandwich colloids of zinc oxide and zinc sulfide in aqueous solutions, *J. Phys. Chem.* 93 (1989) 7707-7713.
- [10] T.P. Radhakrishnan, A. Patra, K. Rajesh, Optical materials based on molecular nano/microcrystals and ultrathin films, *Bull. Mater. Sci.* 31 (2008) 421-427.
- [11] P.S. Subbarao, Y. Aparna, K.V.E. Rao, Proceedings of the 2<sup>nd</sup> international conference on environment science and biotechnology, IACSIT Press, Singapore, 2012.
- [12] X.H. Jia, H.Q. Fan, F.Q. Zhang, L. Qin, Using sonochemistry for the fabrication of hollow ZnO microspheres, *Ultrason. Sonochem.* 17 (2010) 284-287.
- [13] V.G. Pol, A. Gedanken, Deposition of gold nanoparticles on silica spheres: A sonochemical approach, *J. Chem. Mater.* 15(5) (2003) 111-118.
- [14] Tao Gao, Taihong Wang, SnO<sub>2</sub> nanobelt/CdS nanoparticle core/shell heterostructures are successfully achieved via a simple sonochemical approach, *Commun.* 22 (2004) 2558-2559.
- [15] Qiuying Li, Yulu Ma, Chuang Mao, Chifei Wu, Grafting modification and structural degradation of multi-walled carbon nanotubes under the effect of ultrasonics sonochemistry, *Ultrason. Sonochem.* 16 (2009) 752-757.
- [16] K.S. Suslick, M.M. Fang, T. Hyeon, Sonochemical synthesis of iron colloids, *J. Am. Chem. Soc.* 118 (1996) 11960-11961.
- [17] S.B. Maddinedi, B.K. Mandal, Peroxidase Like activity of quinic acid stabilized copper oxide nanosheets, *Austin J. Anal. Pharm. Chem.* 1(2) (2014) 1008-1011.
- [18] I. Prakash, P.N. Muralidharan, M. Nallamuthu, Venkateswarlu, N. Satyanarayana, Nanocrystallite size cuprous oxide: Characterization of copper nanopowders after natural aging, *Mater. Res. Bull.* 42 (2007) 1619-1624.
- [19] Y.C. Zhang, J.Y. Tang, G.L. Wang, M. Zhang and X.Y. Hu, Tailor the crystal shape in high-temperature solution resulted in a simultaneous growth of CuO and Cu<sub>2</sub>O, *J. Cryst. Growth* 294 (2006) 278-282.
- [20] M. Kosmulski, pH-dependent surface charging and points of zero charge II Update, *J. Colloid Interf. Sci.* 275 (2004) 214-224.
- [21] Sathish Mohan Botsa, Ramadevi Dharmasoth, Keloth Basavaiah, A facile synthesis of Cu<sub>2</sub>O and CuO nanoparticles via sonochemical assisted method, *Curr. Nanosci.* 14 (2018) 1-5.
- [22] D. Chen, K. Wang, D. Xiang, R. Zong, W. Yao, Y. Zhu, Significantly enhancement of photocatalytic performances via core-shell structure of ZnO@mpg-C<sub>3</sub>N<sub>4</sub>, *Appl. Catal. B Environ.* 147 (2014) 554-561.
- [23] G. Ren, D. Hu, E.W. Cheng, M.A. Vargas Reus, P. Reip, R.P. Allaker, Characterisation of copper oxide nanoparticles for antimicrobial applications, *Int. J. Antimicrobial Agents* 33 (2009) 587-590.
- [24] P. Cronholm, H.L. Karlsson, J. Hedberg, Intracellular uptake and toxicity of Ag and CuO nanoparticles: A comparison between nanoparticles and their corresponding metal ions, *Small* 9 (2013) 970-982.
- [25] P.K. Stoimenov, R.L. Klinger, G.L. Marchin, Metal oxide nanoparticles as bacterial agents, *Langmuir* 18 (2002) 6679-6686.